A transferable tight-binding potential for carbon

A transferable tight-binding potential for carbon

C H Xu, C Z Wang, C T Chan and K M Ho

Ames Laboratory-USDOE, and Department of Physics and Microelectronics Research Center, Iowa State University, Ames, IA 50011, USA

Abstract. An interatomic potential for carbon is developed that is based on an empirical tight-binding approach. The model reproduces accurately the energy-versus-volume diagram of carbon polytypes and gives a good description of the phonons and elastic constants for carbon in the diamond and graphite structures. To test the transferability of the model to different atomic environments further, we performed molecular-dynamics simulations to study the liquid phase and the properties of small carbon microclusters. The results obtained are in good agreement with those obtained from *ab initio* calculations.

Carbon is unique among the elements in its ability to form strong chemical bonds with a variety of coordination numbers from two (e.g. linear chains or carbyne phase), to three (e.g. graphite) and four (e.g. diamond). Combining strong bonds with light mass and high melting point, condensed carbon phases have many unique properties that make them technologically important as well as scientifically fascinating. Despite extensive studies over the past few decades, many interesting problems remain unresolved—examples including those of the high-temperature, high-pressure phase diagram of carbon [1] and the geometric and electronic structure of various disordered carbon phases [1, 2]. In particular, the recent exciting discovery of carbon fullerenes [3, 4] opened up an entirely new area of research with many unanswered questions.

Previous theoretical studies on condensed carbon fell into two main categories: calculations using *ab initio* techniques [5–9] and calculations based on empirical interatomic potentials [10–16]. In the last ten years, accurate and reliable results have been obtained for the various bulk crystalline phases by first-principles calculations using density-functional theory within the local-density approximation (LDA) [5, 6]. Results for small carbon clusters are also available from accurate Hartree–Fock calculations [7]. Recently, *ab initio* molecular-dynamics simulation of liquid and amorphous carbon with 54 atoms have been carried out using the Car–Parrinello method [8, 9]. Nevertheless, first-principles studies are at present still limited by their heavy demand on computational effort. On the other hand, there have been numerous efforts [10–16] to find an accurate model for the interatomic interactions in carbon, starting from the early work of Born [10] to the recent work of Tersoff [13]. Most of these models [10–13] are classical in nature and cannot account for quantum mechanical effects of the bonding in carbon systems. An alternative approach is·to include the effects of directional covalent bonding through the underlying electronic structure described by an empirical tight-binding (TB) Hamiltonian. Such a scheme allows the quantum

mechanical nature of the covalent bonding to enter the potential in a natural way rather than through the addition of *ad hoc* angular terms in classial potentials. Early versions of TB potentials [14–16] were quite successful in describing the properties of the solid when it is near the diamond structure. However, these early TB models can be quite unreliable when extrapolated to other crystalline or disordered structures. It is clear that the usefulness of a TB model in describing the disordered carbon complex systems is closely related to its transferability. Recently, Goodwin, Skinner and Pettifor (GSP) [17] and Sawada [18] have shown that it is possible to obtain a TB model for Si that accurately describes the energy-versus-volume behaviour of Si in crystalline phases with different atomic coordination as well as the structure of small clusters. This corrects the deficiency in earlier TB models.

In this paper, we develop for carbon a similar TB interatomic potential in which we adopt the scaling form given by Goodwin *et al* [17] for the dependence of the TB hopping parameters and the pairwise potential on the interatomic separation. The model is shown to have good transferability when applied to a wide variety of crystal structures. Applications in molecular-dynamics studies of the liquid phase of carbon as well as the structures of small carbon clusters indicate that the potential does a good job in describing carbon systems over a wide range of environments.

In our model the total energy of the system is written as

$$E_{\text{tot}} = E_{\text{bs}} + E_{\text{rep}} \tag{1}$$

where E_{bs} is the sum of electronic eigenvalues over all occupied electronic states, and E_{rep} is a short-ranged repulsive energy. The electronic eigenvalues are obtained by solving an empirical tight-binding Hamiltonian H_{TB}. The off-diagonal elements of H_{TB} are described by a set of orthogonal sp^3 two-centre hopping parameters, $V_{ss\sigma}$, $V_{sp\sigma}$, $V_{pp\sigma}$ and $V_{pp\pi}$, scaled with interatomic separation r as a function $s(r)$; and the on-site elements are the atomic orbital energies of the corresponding atom. The remainder of E_{tot} is modelled by a short-ranged repulsive term E_{rep} given by

$$E_{\text{rep}} = \sum_i f\left(\sum_j \phi(r_{ij})\right) \tag{2}$$

where $\phi(r_{ij})$ is a pairwise potential between atoms i and j, and f is a functional expressed as a 4th-order polynomial with argument $\sum_j \phi(r_{ij})$.

We adopt the functional form suggested by GSP [17] for the scaling function $s(r)$ and the pairwise potential $\phi(r)$:

$$s(r) = (r_0/r)^n \exp\{n[-(r/r_c)^{n_c} + (r_0/r_c)^{n_c}]\} \tag{3}$$

$$\phi(r) = \phi_0(d_0/r)^m \exp\{m[-(r/d_c)^{m_c} + (d_0/d_c)^{m_c}]\} \tag{4}$$

where r_0 denotes the nearest-neighbour atomic separations in diamond, and $n, n_c, r_c, \phi_0, m, d_c$ and m_c are parameters that need to be determined.

Unlike in the GSP model, the scaling parameters r_c and n_c for $s(r)$ are not necessarily the same as the corresponding d_c and m_c for $\phi(r)$ in our model. Moreover, for the convenience of molecular-dynamics simulation, we require the scaling function $s(r)$ and the pair potential $\phi(r)$ to go smoothly to zero at some designated cut-off distance. This is achieved by replacing the tail of $s(r)$ with a third-order polynomial

$t_s(r-r_1)$ whose coefficients are determined by requiring the connection of $s(r)$ and $t_s(r)$ at r_1 (match point, $r_1 \leqslant r_m$) to be smooth up to the first derivative, and $t_s(r)$ and its first derivative to be zero at r_m. The same procedure is used to determine $t_\phi(r - d_1)$, which replaces the tail of $\phi(r)$.

We chose the cut-off distance r_m and d_m to be 2.6 Å, which is between the nearest-neighbour and next-nearest-neighbour distances of carbon atoms in the diamond structure at equilibrium . The parameters in the model are chosen primarily by fitting first-principles LDA results of energy versus nearest-neighbour interatomic separation for different carbon polytypes [5, 6], i.e. diamond, graphite, linear chain, simple cubic and face-centred cubic structures, with special emphasis on the diamond, graphite and linear chain structures. Additional checks have also been made to ensure that the model gives reasonable results for the electronic band structure, elastic moduli and phonon frequencies in the diamond and graphite structures, although these properties do not enter explicitly into the fitting procedure.

The resulting sp^3 tight-binding parameters are: $E_s = -2.99$ eV, $E_p = 3.71$ eV, $V_{ss\sigma} = -5.0$ eV, $V_{sp\sigma} = 4.7$ eV, $V_{pp\sigma} = 5.5$ eV and $V_{pp\pi} = -1.55$ eV. The parameters for $s(r)$ and $\phi(r)$, the coefficients for the tail functions $t_s(r - r_1)$ and $t_\phi(r-d_1)$, and the coefficients for the polynomial function $f(x) = \sum_{n=0}^{4} c_n x^n$, with $x = \sum_j \phi(r_{ij})$ are given in table 1 and table 2 respectively.

Table 1. Parameters for the functions $s(r)$ and $\phi(r)$. See equations (3), (4) and the text for details.

n	n_c	r_c (Å)	r_0 (Å)	r_1 (Å)	
2.0	6.5	2.18	1.536 329	2.45	
ϕ_0 (eV)	m	m_c	d_c (Å)	d_0 (Å)	d_1 (Å)
8.185 55	3.303 04	8.6655	2.1052	1.64	2.57

Table 2. Coefficients of the polynomial functions $t_s(r - r_1)$, $t_\phi(r - d_1)$, and $f(x)$. See also the text for details.

	$t_s(r - r_1)$	$t_\phi(r - d_1)$	$f(x)$
c_0	$6.739\,262\,007\,431\,4 \times 10^{-3}$	$2.250\,429\,010\,9 \times 10^{-8}$	$-2.590\,976\,511\,819\,1$
c_1	$-8.188\,535\,951\,789\,8 \times 10^{-2}$	$-1.440\,864\,056\,1 \times 10^{-6}$	$0.572\,115\,149\,861\,9$
c_2	$0.193\,236\,525\,914\,4$	$2.104\,330\,337\,4 \times 10^{-5}$	$-1.789\,634\,990\,399\,6 \times 10^{-3}$
c_3	$0.354\,287\,433\,238\,0$	$6.602\,439\,022\,6 \times 10^{-5}$	$2.353\,922\,151\,675\,7 \times 10^{-5}$
c_4			$-1.242\,511\,695\,515\,87 \times 10^{-7}$

As one sees from figure 1, these parameters reproduce excellently the energy curves of the two most stable structures, i.e. graphite and diamond. The energy curve of the linear chain is also adequately described. Although the model does not predict well the curvatures of the energy curves for more highly coordinated structures, it does yield reasonably good cohesive energies and equilibrium volumes for these structures in comparison with the results of LDA calculations [5, 6]. Such a comparison is shown in figures 2 and 3.

In table 3, the vibrational and elastic properties of diamond predicted by the present TB model are presented and compared with experimental data [19]. Very
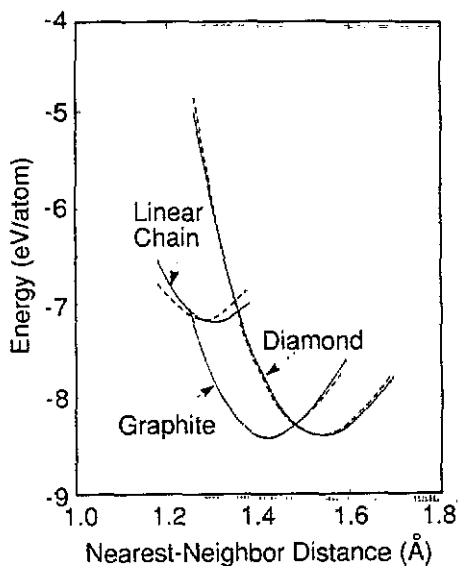
Figure 1. Cohesive energy against nearest-neighbour atomic distance for carbon in the diamond, graphite, and linear chain structures. Solid and dashed lines show the results from TB calculations and LDA calculations, respectively. The LDA data of diamond are from [5] and those of graphite and linear chain are from [6].
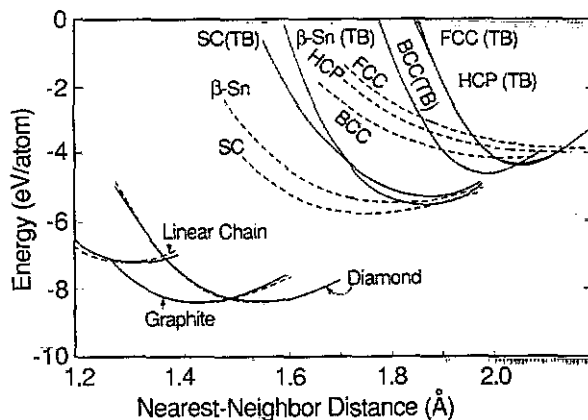

Figure 2. Cohesive energy against nearest-neighbour atomic distance curves for the diamond, graphite, linear chain, SC, β-Sn, BCC, HCP and FCC structures. Full and broken lines show the results from tight-binding calculations and LDA calculations, respectively. The LDA data are from [5] and [6].

good agreement is achieved between our calculated phonon frequencies and the experimental data [19] (errors all within 10%) particularly considering that the phonon frequencies are not included explicitly into the fitting bases. However, the elastic constants $C_{11} - C_{12}$ and C_{44} are too soft in comparison with experimental data.

We have also tested the elastic constants and phonons for graphite. The graphite structure was considered as just a two-dimensional layer in our study, since the interlayer spacing of graphite is much larger than the cut-off distance of our TB potential. The calculated phonon frequencies for the E_{2g_2} and A_{2u} modes are $\nu_{TO}(E_{2g_2}) = 1664.0$ cm^{-1} and $\nu_{TO}(A_{2u}) = 973.2$ cm^{-1}, which are sufficiently close to the experimental values 1582.0 cm^{-1} and 868.0 cm^{-1} [20]. The elastic
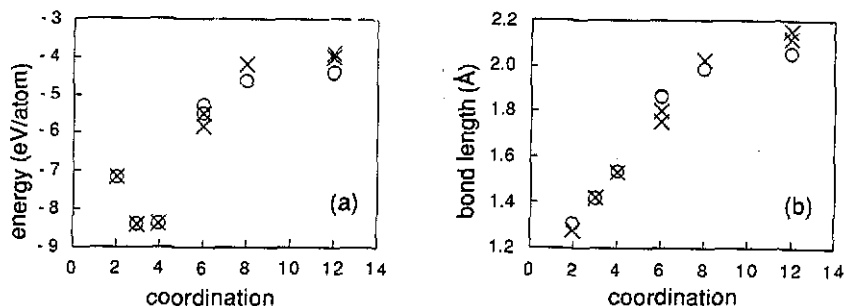
Figure 3. (*a*) Cohesive energy and (*b*) bond length of carbon as a function of coordination number. The results from the present TB calculation (the open circles) are in good agreement with those obtained by the first-principles LDA calculations (the crosses, quoted from [5] and [6]).

Table 3. Elastic constants, phonon frequencies and Grüneisen parameters of diamond calculated from the present TB model are compared with experimental results (from [19]). Elastic constants are in units of 10^{12} dyn cm^{-2} and the phonon frequencies are in tHz.

	Model	Experiment
$c_{11} - c_{12}$	6.22	9.51
c_{44}^0	5.42	
c_{44}	4.75	5.76
$\nu_{LTO(\Gamma)}$	37.80	39.90
$\nu_{TA(X)}$	22.42	24.20
$\nu_{TO(X)}$	33.75	32.0
$\nu_{LA(X)}$	34.75	35.5
$\gamma_{LTO(\Gamma)}$	1.03	0.96
$\gamma_{TA(X)}$	−0.16	
$\gamma_{TO(X)}$	1.10	
$\gamma_{LA(X)}$	0.62	

constants of graphite are also in very good agreement with experimental data (see table 4).

Table 4. Elastic constants, phonon frequencies and Grüneisen parameters of graphite calculated from the present TB model are compared with experimental results (from [20]). Elastic constants are in units of 10^{12} dyn cm^{-2} and the phonon frequencies are in tHz.

	Model	Experiment
$c_{11} - c_{12}$	8.40	8.80
E_{2g_2}	49.92	47.46
A_{2u}	29.19	26.04
$\gamma(E_{2g_2})$	2.00	
$\gamma(A_{2u})$	0.10	

To test the transferability of the model to different atomic environments further, we used the model in molecular dynamics [21] to study the structural properties of liquid carbon and small carbon clusters.

The simulation of liquid carbon is performed with 54 atoms and with FCC periodic boundary conditions, to compare directly with recent *ab initio* molecular-dynamics simulation using the Car–Parrinello method [9]. The density of the sample is chosen to be 2.0 g cm^{-3} according to [9] and the MD cell is fixed in volume and shape. The time step used to solve the equation of motion is 0.7×10^{-15} s, about ten times larger than that used in the Car–Parrinello simulation. After 6000 MD steps of thermal equilibration at a temperature of about 5000 K, a statistical average of structural properties is computed over an additional 10 000 MD steps (corresponding to 7.0 ps). The radial distribution function $g(r)$ obtained from our simulation (plotted in figure 4) is found to be in good agreement with that obtained by *ab initio* molecular dynamics [9].
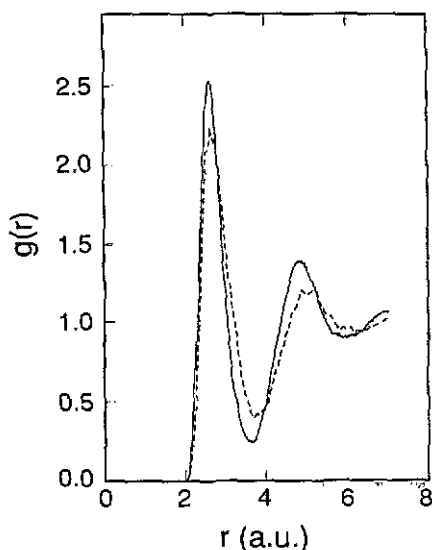

Figure 4. Radial distribution function $g(r)$ of liquid carbon. The full line is the present TB molecular-dynamics result and the broken line is the result from *ab initio* molecular dynamics (from [9]).
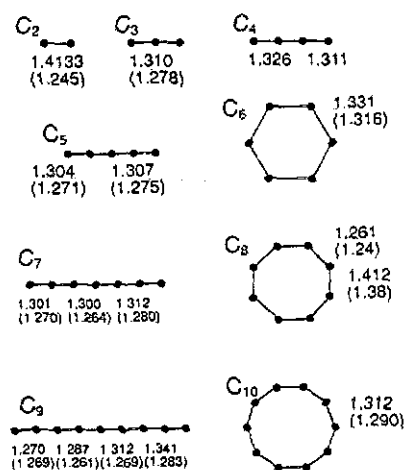
Figure 5. The ground-state geometries of carbon clusters $C_2 - C_{10}$ from our TB calculation. The numbers show the corresponding bond lengths. *Ab initio* calculation results of bond lengths from [7] are also shown in the parentheses for comparison. Bond lengths are in units of Å.

The ground-state geometries of small carbon clusters C_n ($n = 2$–10) are studied by simulated annealing using molecular dynamics with the present TB potential. In order to handle the effects of charge transfer in such small systems correctly, particularly in the presence of dangling bonds, we have added a Hubbard-like term [22]

$$H_u = \tfrac{1}{2} u (q_i - q_i^0)^2 \qquad (5)$$

to the TB Hamiltonian H_{TB}, where q_i is the Mulliken population at atomic site i; q_i^0 is 4 for sp^3 TB orbitals. The parameter u is taken to be 4 eV. Both a linear chain and a monocyclic ring structure were used as starting configurations for the simulation. After careful annealing, each of the clusters converged to a unique

final structure regardless of its initial configurations. These ground-state structures are shown in figure 5. In the range $5 \leqslant n \leqslant 10$, we found that odd-numbered clusters prefer a linear structure, while even-numbered clusters prefer a ring structure. This result agrees well with the accurate *ab initio* Hartree–Fock calculation result of Raghavachari *et al* [7]. For the very small clusters ($n \leqslant 4$), the linear chain structure is found to be the most stable geometry. Thus, except for in the case of $n = 4$, the geometries obtained from our model agree completely with those from accurate *ab initio* quantum calculations. Since the potential parameters are determined by fitting to bulk properties, we expect that our model will become even more reliable as the cluster size gets bigger.

In conclusion, our TB approach gives an accurate description of the atomic interactions in carbon systems. It is able to reproduce the energy–volume curves of accurate LDA calculations, with excellent transferability among the graphite, diamond and linear chain structures. The model gives a good description of the dynamical and elastic properties of graphite and diamond. Applications of the model to the molecular-dynamics simulation of clusters and liquid carbon yields results that agree well with those from accurate *ab initio* calculations. We expect that our model potential will have widespread applications in the study of complex carbon systems.

References

[1] Bundy F P 1989 *Physica* A **156** 169 and references therein
[2] Robertson J 1986 *Adv. Phy.* **35** 317 and references therein
[3] Kroto H W, Heath J R, O'Brien S C, Curl R F and Smalley R E 1985 *Nature* **318** 162
[4] Krätschmer W, Lamb L D, Fostiropoulos K and Huffman D R 1990 *Nature* **347** 354
[5] Fahy S and Louie S G 1987 *Phys. Rev.* B **36** 3373
[6] Chan C T 1989 unpublished
[7] Raghavachari K and Binkley J S 1987 *J. Chem. Phys.* **87** 2191
[8] Galli G, Martin R M, Car R and Parrinello M 1989 *Phys. Rev. Lett.* **62** 555
[9] Galli G, Martin R M, Car R and Parrinello M 1989 *Phys. Rev. Lett.* **63** 988
[10] Born M 1914 *Ann. Phys., Lpz.* **44** 605
[11] Cochran W 1959 *Proc. R. Soc.* A **253** 260
[12] Weber W 1974 *Phys. Rev. Lett.* **33** 371; 1977 *Phys. Rev.* B **15** 4789
[13] Tersoff J 1988 *Phys. Rev. Lett.* **61** 2879
[14] Chadi D J and Martin R M 1976 *Solid State Commun.* **19** 643
[15] Harrison W A 1980 *Electronic Structure and the Properties of Solids* (San Fransisco: Freeman)
[16] Wang C Z, Chan C T and Ho K M 1990 *Phys. Rev.* B **42** 11 276
[17] Goodwin L, Skinner A J and Pettifor D G 1989 *Europhys. Lett.* **9** 701
[18] Sawada S 1990 *Vacuum* **41** 612
[19] 1987 *Semiconductors: Intrinsic Properties of Group IV Elements and III–V, II–VI, and I–VII Compounds* ed O Madelung *et al* (Berlin: Spring) and references therein
1982 *Semiconductors: Physics of Group IV Elements and III–V Compounds* ed O Madelung *et al* (Berlin: Springer) and references therein

[20] Dresselhaus M S and Dresselhaus G 1982 *Light Scattering in Solids III* ed M Cardona and G
       Güntherodt (Berlin: Springer) p 9
[21] For details of molecular dynamics using a TB potential model, see
       Wang C Z, Chan C T and Ho K M 1989 *Phys. Rev.* B **39** 8586
[22] A comparison of the results from the TB model with H_u and from the TB model without H_u showed
       that the effects of the Hubbard term are significant only for small clusters of size $n \leqslant 11$.